

Magnetic properties of Co/Ni-based multilayers with Pd and Pt insertion layers

M. Heigl,* R. Wendler, S. Haugg, and M. Albrecht

(Dated: May 23, 2022)

In this study, the influence of Pd and Pt insertion layers in Co/Ni multilayers (MLs) on their magnetic properties, e.g. magnetic anisotropies, saturation magnetization, coercivity, magnetic domain size, and Curie temperature, is investigated. We compare three series of $[\text{Co}/\text{Ni}/\text{X}]_N$ ML systems ($X = \text{Pd}, \text{Pt}$, no insertion layer), varying the individual Co layer thickness as well as the repetition number N . All three systems behave very similarly for the different Co layer thicknesses. For all systems, a maximum effective magnetic anisotropy was achieved for MLs with a Co layer thickness between 0.15 nm and 0.25 nm. The transition from an out-of-plane to an in-plane system occurs at about 0.4 nm of Co. While $[\text{Co}(0.2 \text{ nm})/\text{Ni}(0.4 \text{ nm})]_N$ MLs change their preferred easy magnetization axis from out-of-plane to in-plane after 6 bilayer repetitions, insertion of Pd and Pt results in an extension of this transition beyond 15 repetitions. The maximum effective magnetic anisotropy was more than doubled from 105 kJ/m^3 for $[\text{Co}/\text{Ni}]_3$ to 275 and 186 kJ/m^3 for Pt and Pd, respectively. Furthermore, the insertion layers strongly reduce the initial saturation magnetization of 1100 kA/m of Co/Ni MLs and lower the Curie temperature from 720 to around 500 K.

I. INTRODUCTION

Magnetic thin film systems with perpendicular magnetic anisotropy (PMA) have been and are still intensively investigated. PMA is displayed in several Co-based multilayered structures [1–8] and was shown to be useful for a variety of applications, including perpendicular magneto-optical recording [9, 10], spin-transfer-torque magneto-resistive random access memories (STT-MRAM)[11–15], domain-wall-motion-based devices [16, 17], bit patterned media [18–21], and biomedical applications [22]. In this regard, Co/Ni multilayers (MLs) are of particular interest because of their additional high spin polarization [23, 24] and low intrinsic Gilbert damping [5, 11, 25–28]. PMA in these MLs is mainly contributed to interface magnetic anisotropy [6–8, 29] and magnetoelastic anisotropy [30–32]. Theoretical calculations predict a maximum PMA for Co/Ni MLs in the fcc(111) structure at a Co thickness of one monolayer and a Ni thickness of two monolayers[7, 33] ($\approx \text{Co}(0.2 \text{ nm})/\text{Ni}(0.4 \text{ nm})$), which has been experimentally confirmed by multiple groups [3, 4, 34–37]. Previous studies have shown that PMA of Co/Ni MLs is strongly affected by the deposition process [38, 39], choice of seed layers[40], and post-treatment processing, e.g. annealing [41, 42] or ion radiation [31, 43]. This limits the feasibility for many applications where the seed layer is not freely selectable or post-deposition treatments are no option. On the other hand, Co/Pt and Co/Pd MLs also exhibit large PMA and are less sensitive to seed layers or sputter-deposition conditions [1, 36, 44–47].

In this work, we combine these systems in order to enhance PMA by adding Pt or Pd insertion layers to Co/Ni MLs. These trilayer-based films provide a highly tunable system for a wide range of applications. A previous study of Ni/Co/Pt and Co/Ni/Pt MLs has already demonstrated enhanced PMA and annealing stability compared to Co/Ni MLs [48]. It has also been shown that the stacking order of the trilayer, as well as the Pt thickness is important. Here, we focus on Pd insertion

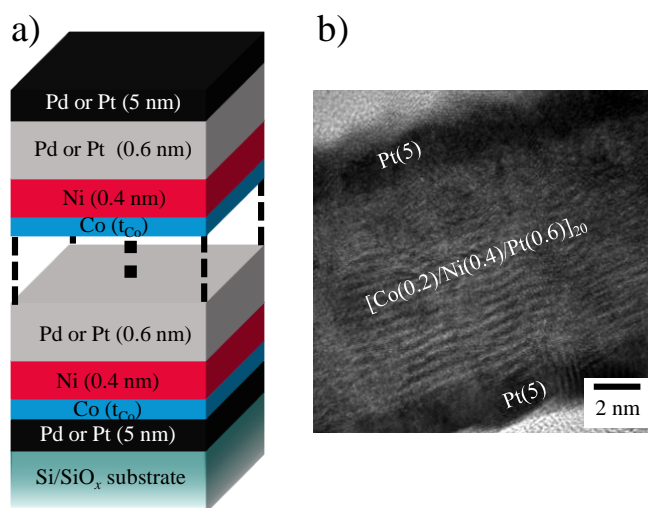


FIG. 1. (a) Schematic image illustrating the layer stacking of Co/Ni/Pd(Pt) MLs. (b) Exemplary cross-section TEM image of a Pt(5 nm)/[Co(0.2 nm)/Ni(0.4 nm)/Pt(0.6 nm)]₂₀/Pt(5 nm) film sample.

layers and investigate their impact on the magnetic properties as a function of ML repetition number and Co layer thicknesses and provide a comparison to Co/Ni and Co/Ni/Pt MLs.

II. EXPERIMENTAL DETAILS

A series of $[\text{Co}(t_{\text{Co}})/\text{Ni}(0.4)/\text{X}(0.6)]_N$ MLs ($X = \text{Pd}, \text{Pt}$, no insertion layer; thicknesses are given in nm) with various repetition numbers N and different individual Co layer thicknesses t_{Co} were investigated. The films were deposited at room temperature by magnetron sputtering (base pressure $< 10^{-8}$ mbar) from elemental targets. The Ar pressure was kept constant at 5×10^{-3} mbar during the deposition process. The individual layer thicknesses were determined using a calibrated deposition rate. The films were prepared on Si(001) substrates with a 100 nm thick thermally oxidized SiO_x layer. 5 nm of Pt were used as seed and capping layer for the Co/Ni

* michael.heigl@physik.uni-augsburg.de.

and Co/Ni/Pt MLs. Accordingly, 5 nm of Pd were used as seed and capping layer for the Co/Ni/Pd MLs.

We fixed the Ni and Pd/Pt layer thickness to 0.4 and 0.6 nm, respectively, and varied the Co layer thicknesses between 0.1 and 0.5 nm. The bi- and trilayers were repeated to form MLs with repetition numbers N between 1 and 15. A schematic of the layer stack is depicted in figure 1 a) along with an exemplary transmission electron microscopy (TEM) cross-section image of a $[\text{Co}(0.2)/\text{Ni}(0.4)/\text{Pt}(0.6)]_{20}$ film sample (figure 1 b), confirming the overall layer structure. Note that it is not possible to differentiate between Co and Ni layers because of their similar atomic number (Z contrast). Thus, only the contrast between two equally thick layers of Co/Ni and Pt is visible.

The integral magnetic properties of the samples were investigated by superconducting quantum interference device-vibrating sample magnetometry (SQUID-VSM). M - $\mu_0 H$ hysteresis loops were measured in out-of-plane (oop) and in-plane (ip) geometry at room temperature. It has been shown that edge effects can lead to artifacts in the measured M - $\mu_0 H$ hysteresis loops [49]. Thus, their occurrence was prevented by cutting all edges of the measured samples. The effective magnetic anisotropy K_{eff} was determined from the integrated area difference between the oop and ip M - $\mu_0 H$ hysteresis loops. Please note that for calculating the saturation magnetization M_s , the total film volume (including the insertion layers) was taken into account. In order to obtain the Curie temperature, the oop or ip remanent magnetization was measured in the temperature range between 300 and 800 K with a magnetic guiding field of 10 mT. Magnetic force microscopy (MFM) was used to receive information about the magnetic domain structure after sample demagnetization at room temperature. In order to access the equilibrium domain size, the samples were demagnetized by decaying alternating magnetic fields.

III. RESULTS AND DISCUSSION

A. Co layer thickness dependence

In a first study, the individual Co layer thickness t_{Co} was varied between 0.1 and 0.5 nm for three sample series, $[\text{Co}(t_{\text{Co}})/\text{Ni}]_3$, $[\text{Co}(t_{\text{Co}})/\text{Ni}/\text{Pd}]_9$, and $[\text{Co}(t_{\text{Co}})/\text{Ni}/\text{Pt}]_4$. The Ni and Pd/Pt thicknesses were set to 0.4 and 0.6 nm, respectively. The repetition numbers were chosen to ensure an oop easy axis at thinner Co thicknesses. In figure 2, exemplary oop and ip M - $\mu_0 H$ hysteresis loops for four different Co layer thicknesses are displayed. Based on the M - $\mu_0 H$ data, the magnetic properties of the three sample series as a function of Co layer thickness were extracted and summarized in figure 3.

The effective magnetic anisotropy K_{eff} consists of the uniaxial magnetic anisotropy K_u and the magnetic shape anisotropy $K_{\text{sh}} = \frac{\mu_0}{2} M_s^2$:

$$K_{\text{eff}} = K_u - \frac{\mu_0}{2} M_s^2. \quad (1)$$

The measured K_{eff} values are displayed in figure 3 a). Positive values of K_{eff} imply an oop easy axis, negative val-

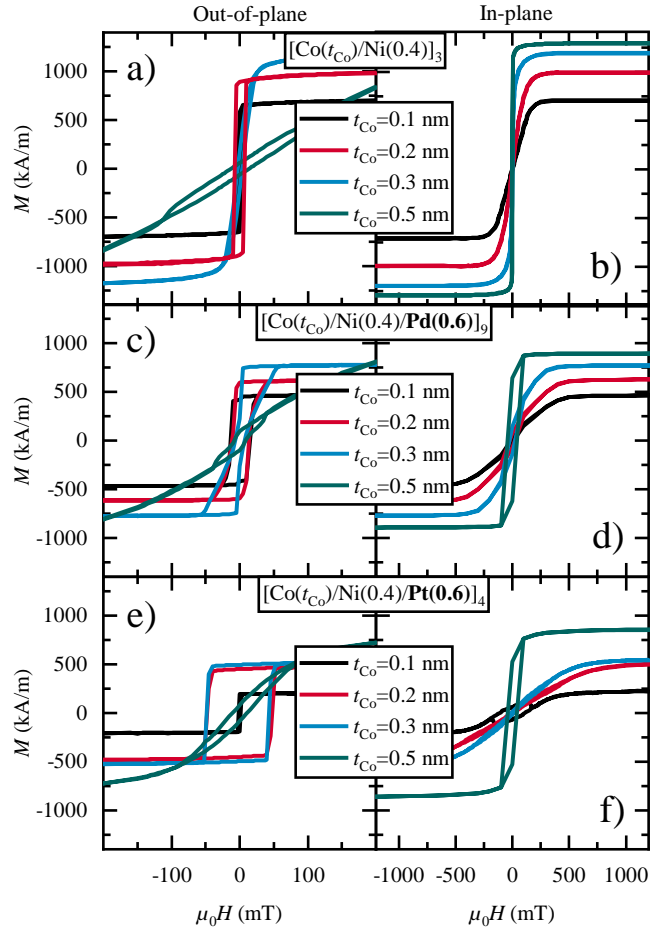


FIG. 2. M - $\mu_0 H$ hysteresis loops obtained in oop and ip geometry of $[\text{Co}(t_{\text{Co}})/\text{Ni}(0.4)]_3$ (a, b), $[\text{Co}(t_{\text{Co}})/\text{Ni}(0.4)/\text{Pd}(0.6)]_9$ (c, d), and $[\text{Co}(t_{\text{Co}})/\text{Ni}(0.4)/\text{Pt}(0.6)]_4$ (e, f) with varying Co layer thickness. (All thicknesses are given in nm)

ues an ip easy axis. If the shape anisotropy is larger than the uniaxial one, a transition from an oop to an ip easy axis occurs. The $[\text{Co}(t_{\text{Co}})/\text{Ni}(0.4)]_3$ series shows a maximum K_{eff} of $70 \pm 7 \text{ kJ/m}^3$ for $0.15 \text{ nm} \leq t_{\text{Co}} < 0.20 \text{ nm}$. For thicker Co layers, K_{eff} decreases and the easy axis direction changes from oop to ip between $0.30 \text{ nm} < t_{\text{Co}} < 0.40 \text{ nm}$. These results confirm previous studies on thickness dependencies in Co/Ni MLs revealing an optimal thickness ratio between Co and Ni of about one to two in order to get high PMA [3, 4, 34–37]. The sample series with insertion layers behave qualitatively similar. All systems have their maximum K_{eff} for a Co layer thickness between 0.15 and 0.25 nm and their easy axis changes to the in-plane orientation at around 0.40 nm. However, in comparison to Co/Ni, the maximum K_{eff} is more than doubled with insertion layers, where $[\text{Co}(0.15)/\text{Ni}(0.4)/\text{Pd}(0.6)]_9$ has a K_{eff} of $173 \pm 17 \text{ kJ/m}^3$ and $[\text{Co}(0.25)/\text{Ni}(0.4)/\text{Pt}(0.6)]_4$ of $201 \pm 20 \text{ kJ/m}^3$. This increase in anisotropy can be mainly attributed to the lower magnetization M_s (see figure 3 c)) and thus a smaller K_{sh} . Additionally, the insertion layer tend to prevent intermixing at the Ni and

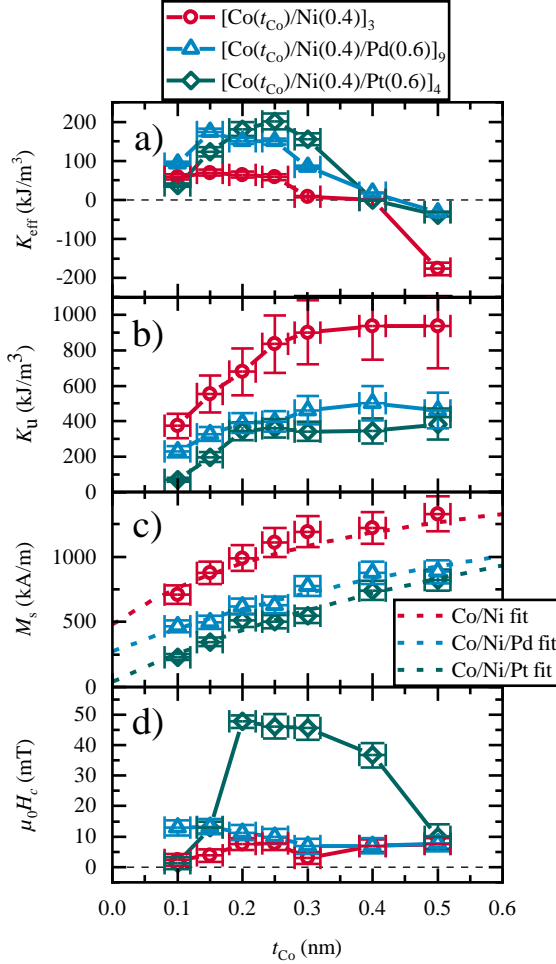


FIG. 3. Effective magnetic anisotropy K_{eff} (a), uniaxial magnetic anisotropy K_u (b), saturation magnetization M_s (c), and coercivity field $\mu_0 H_c$ (d) as function of Co layer thickness t_{Co} . (All thicknesses are given in nm)

Co interface, which might give rise to an increased interface magnetic anisotropy [17, 40, 50].

Generally, K_u mainly arises from interface effects in these systems [6–8, 29]. Thus, K_u should not be thickness-dependent. This is only observable in figure 3 b) for $t_{Co} > 0.2$ nm, where K_u saturates for all systems. Below this thickness, the Co layer is particularly influenced by roughness and non-continuous growth. Co/Ni MLs show larger K_u values despite the lower interface anisotropy terms of Co/Ni (0.31 mJ/m²) [7] in comparison to Co/Pt (0.50 mJ/m²) [6] and Co/Pd (0.40 mJ/m²) [6]. This can be explained by the higher number of interfaces per thickness. While Co(0.2)/Ni(0.4) MLs have 3 interfaces per 1.2 nm of film, Co(0.2)/Ni(0.4)/X(0.6) MLs contain only 2. Additionally, the smaller amount of repetitions increases the impact of the interfaces to the Pt and Pd seed and capping layer.

The saturation magnetization M_s of all systems displayed in figure 3 c) increases with Co layer thickness. The behavior of [Co(t_{Co})/Ni(0.4)]₃ can be modeled by a linear combination of

two individual magnetization contributions:

$$M_s = \frac{t_{Co}M_{s,Co} + 0.4M_{s,Ni}}{t_{Co} + 0.4} \quad (2)$$

The magnetizations of the Co layer $M_{s,Co}$ and Ni layer $M_{s,Ni}$ were chosen as fit parameters. The measured data and fit can be seen in figure 3 c). $M_{s,Co}$ has the fit value 1892 kA/m. It exceeds the bulk value of 1440 kA/m [51], which can be explained by the higher magnetization of ultra-thin Co films [52] and the increasing polarization of the Pt seed layer with Co layer thickness. D. Weller et al. showed that there is no additional magnetic moment enhancement for Co/Ni interfaces. [53]. The fit value of $M_{s,Ni} = 480$ kA/m agrees well with the bulk value of 488 kA/m [51]. The magnetization of the MLs with insertion layers X can be fitted in a similar way:

$$M_s = \frac{t_{Co}M_{s,Co+X} + (0.4 + 0.6)M_{s,Ni+X}}{t_{Co} + 0.4 + 0.6} \quad (3)$$

For this fit, the polarization of the insertion layer is included both in the t_{Co} -dependent, as well as the t_{Co} -independent term. The fit parameter $M_{s,Co+X}$ for Co(t_{Co})/Ni(0.4)/Pd(0.6) converges at 2231 kA/m. This increase in magnetization compared to bulk Co can mainly be explained by the polarization of Pd, which is dependent on t_{Co} in the analyzed thickness range [30]. The t_{Co} -independent fit parameter $M_{s,Ni+X}$ for Co/Ni/Pd equals 272 kA/m. Beside the magnetization of the Ni layer, the Pd layer polarized by Co [30] and Ni [54] contributes. The measured values of [Co(t_{Co})/Ni(0.4)/Pt(0.6)]₄ lead to the fit parameters $M_{s,Co+X} = 2413$ kA/m and $M_{s,Ni+X} = 40$ kA/m. The high value of $M_{s,Co+X}$ is again due to the polarization of Pt by Co []. The interface between Ni and Pt is known to form a nonmagnetic NiPt alloy [55], which leads to an effectively lower magnetization for the Ni and Pt layers. If we compare the two insertion layers magnetization-wise, it is important to note that the repetition number of [Co(t_{Co})/Ni(0.4)/Pt(0.6)]₄ is lower than that of [Co(t_{Co})/Ni(0.4)/Pd(0.6)]₉. Despite that, Pd generally shows a slightly larger induced magnetization which is less dependent on the Co layer thickness. The same observation was made in reference [53] where Co/Pd and Co/Pt MLs were compared. It was reported that Co/Pd MLs exhibit a magnetization value 15% larger than that of Co/Pt MLs due to enhanced orbital moment of Co and larger polarization of Pd.

Figure 3 d) shows the coercivity field $\mu_0 H_c$ of the oop hysteresis loops for the three sample series. The increase up to $t_{Co} = 0.2$ nm can again be explained by the roughness of the sample and non-continuous growth of the Co layer. All sample series have their maximum at around 0.2 nm with the highest value obtained for the [Co/Ni/Pt]₄ ML.

B. Multilayer repetition dependence

In a further study, we investigated the dependence on the repetition number N for the following three sample

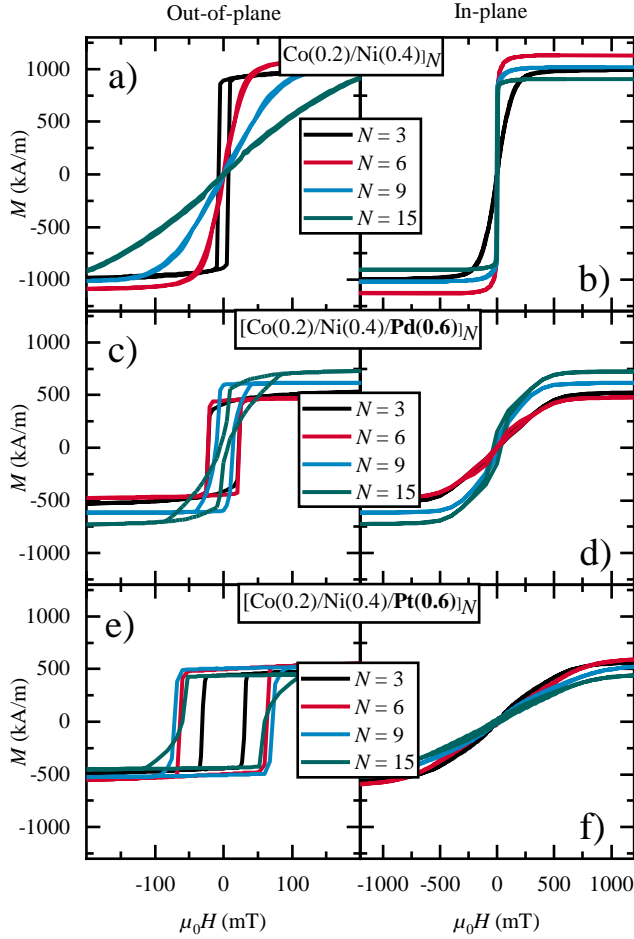


FIG. 4. M - μ_0H hysteresis loops obtained in oop and ip geometry of the three sample series with varying repetition number N . (All thicknesses are given in nm)

series: $[\text{Co}(0.2)/\text{Ni}(0.4)]_N$, $[\text{Co}(0.2)/\text{Ni}(0.4)/\text{Pd}(0.6)]_N$, and $[\text{Co}(0.2)/\text{Ni}(0.4)/\text{Pt}(0.6)]_N$. Based on the results of the Co layer thickness study in section III A, $t_{\text{Co}} = 0.2$ nm was selected for all films. The thicknesses of Ni and Pd/Pt stayed fixed at 0.4 and 0.6 nm, respectively. Figure 4 shows exemplary oop and ip M - μ_0H hysteresis loops of the three sample series. Based on the M - μ_0H data, the magnetic properties of the three sample series as a function of repetition number were extracted and summarized in figure 5.

In figure 5 a), the behavior of K_{eff} for $N \leq 2$ can be explained by the onset of superparamagnetism in ultra-thin films [56]. The values of K_{eff} in Co/Ni MLs change sign between $N = 5$ and $N = 6$ and with it their easy axes transition from oop to ip direction, which is mainly the result of increasing M_s and later of decreasing K_u . There are two widely investigated approaches to delay this transition up to 10 repetitions: (i) increasing K_u by annealing [8] and seed layer optimization [8], or (ii) decreasing M_s (K_{sh}) by changing the ratio of Ni to Co [8]. Introducing a paramagnetic insertion layer does both. The magnetization is reduced and the intermixing and roughness decreases [17, 40, 50]. This leads to a contrary behavior

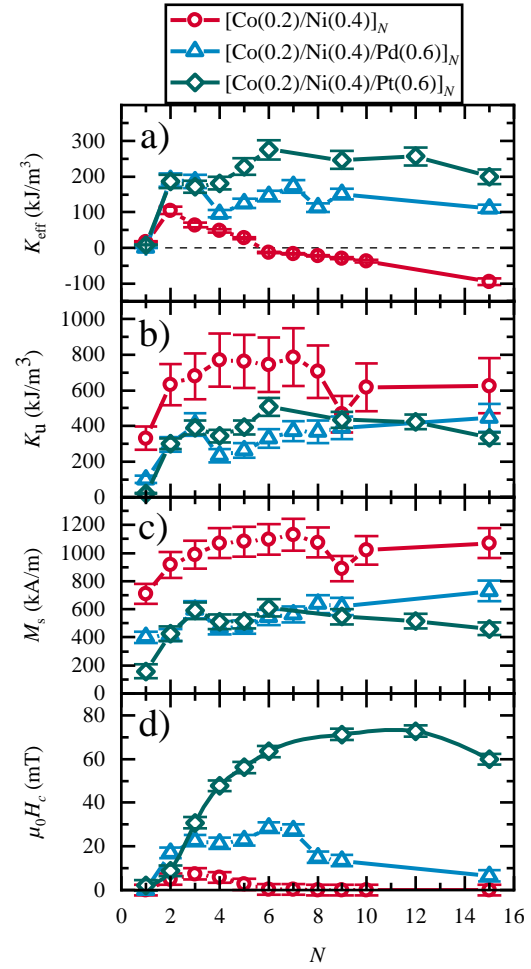


FIG. 5. Effective anisotropy K_{eff} (a), Uniaxial anisotropy K_u (b), saturation magnetization M_s (c), and coercivity field μ_0H_c (d) as function of repetition number N . (All thicknesses are given in nm)

of K_{eff} in Co/Ni/X MLs: their K_{eff} values stay mostly constant within the studied repetition numbers. It was also possible to increase the maximum effective magnetic anisotropy more than twofold from $105 \pm 10 \text{ kJ/m}^3$ for $[\text{Co}/\text{Ni}]_3$ to $186 \pm 19 \text{ kJ/m}^3$ for $[\text{Co}/\text{Ni}/\text{Pd}]_3$ and $275 \pm 28 \text{ kJ/m}^3$ for $[\text{Co}/\text{Ni}/\text{Pt}]_6$.

The K_u values shown in figure 5 b) increase for the Co/Ni MLs up to 4 repetitions to a maximum value of about $780 \pm 162 \text{ kJ/m}^3$ and after 7 repetitions it starts to get reduced. The large error bars arise from the quadratic error propagation of M_s . The behavior and values are in good agreement with recent work of Arora et al. [8]. They showed that the moderate decrease of K_u for $N \geq 10$ can be explained by increasing roughness and intermixing with larger N . The decrease for repetition numbers below 3 can be again explained by the onset of superparamagnetism. We observe a similar behavior for the sample series with insertion layers. The maximum K_u value of $[\text{Co}/\text{Ni}/\text{Pd}]_{15}$ and $[\text{Co}/\text{Ni}/\text{Pt}]_6$ amounts to $445 \pm 78 \text{ kJ/m}^3$ and $507 \pm 51 \text{ kJ/m}^3$, respectively, which is relatively small compared to $780 \pm 162 \text{ kJ/m}^3$ of $[\text{Co}/\text{Ni}]_7$.

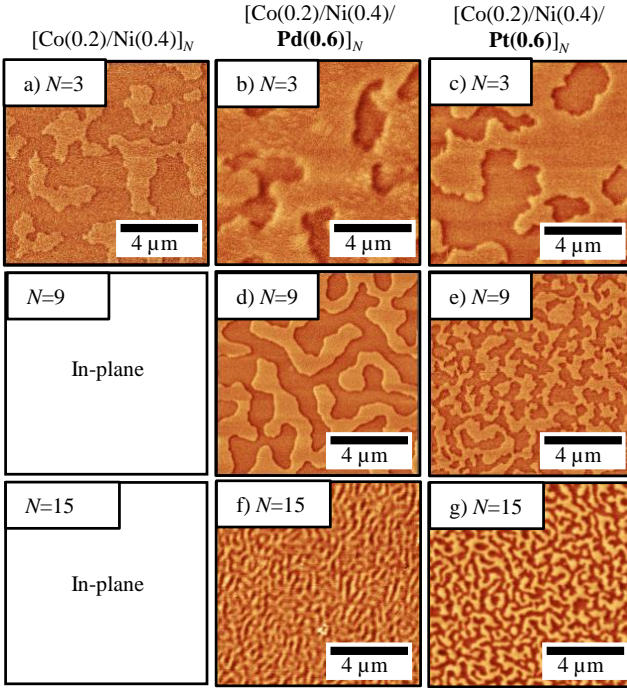


FIG. 6. Magnetic force microscopy images of $[\text{Co}(0.2)/\text{Ni}(0.4)]_N$ (a), $[\text{Co}(0.2)/\text{Ni}(0.4)/\text{Pd}(0.6)]_N$ (b, d, f), and $[\text{Co}(0.2)/\text{Ni}(0.4)/\text{Pt}(0.6)]_N$ (c, e, g) after sample demagnetization. (All thicknesses are given in nm)

The ratio of the M_s values between the three sample series shown in figure 5c) stays more or less the same as already described in section III A. Moreover, we can observe superparamagnetic behavior in all three systems for low N , which is also apparent in the coercivity values $\mu_0 H_c$ (figure 5 d).

In addition, we investigated the equilibrium domain size by MFM after demagnetizing the samples. Figure 6 shows MFM images of the three sample series with different repetition numbers. It was not possible to measure images of $[\text{Co}(0.2)/\text{Ni}(0.4)]_N$ for $N=9$ and 15 due to the ip orientation of the easy axis. Theoretically, the magnetic domain size depends on the ratio D_0 of the domain wall and magnetostatic energies in the following way [57]:

$$D_0 = \frac{4\pi(AK_u)^{1/2}}{\mu_0 M_s^2}, \quad (4)$$

whereas A is the magnetic exchange stiffness. The magnetic domain size D can be estimated depending on the total film thickness t by

$$D(t) \propto t \cdot \exp\left(\frac{D_0}{t}\right). \quad (5)$$

D has its minimum at $t = D_0$ in equation 5. For $t < D_0$, D decreases rapidly with increasing t . $[\text{Co}/\text{Ni}]_3$ has the smallest D_0 of the analyzed samples. For Co/Ni MLs an exchange stiffness of $A \approx 10^{-11} \text{ J/m}$ is commonly assumed[58].

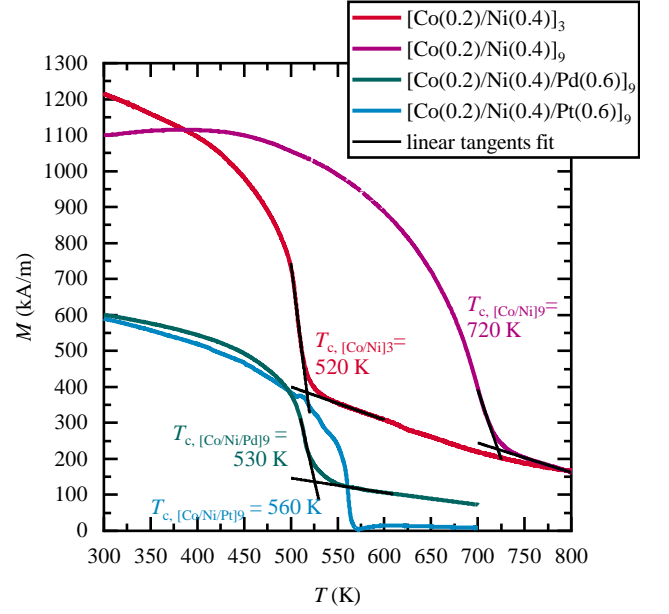


FIG. 7. Magnetization M against temperature T curve with a guiding field of 10 mT. The Curie temperatures were estimated by linear fits around the turning point. (All thicknesses are given in nm)

If we estimate D_0 with this value, we get $D_0 \approx 30 \text{ nm}$ for $[\text{Co}(0.2)/\text{Ni}(0.4)]_3$. Thus, for all sample series the domain sizes decrease with higher repetition number (total thicknesses t). Please note that a direct comparison of the measured domain sizes with its theoretical estimation is hardly possible due to the exponential dependency of equation 5 and the error range of the measured magnetic properties. Thus, in the following, the evolution of the domain sizes for the sample series is discussed only qualitatively. In the first row of figure 6 a-c) the domain sizes of MLs with $N = 3$ are quite similar despite of the differences in measured magnetic properties between Co/Ni and Co/Ni/X (see figure 5). The larger K_u and smaller t values of $[\text{Co}/\text{Ni}]_3$ are offset by the larger M_s in equations 4 and 5. For larger repetition numbers, we can only compare the films with insertion layers. As already mentioned, the domain size is expected to decrease with increasing film thickness (for $t < D_0$), which is also observed in figure 6 b), d), f) for Co/Ni/Pd and c), e), g) for Co/Ni/Pt. A similar behavior was already reported for Co/Ni[59, 60] and for Co/Pt[61] MLs. Despite a smaller K_u and larger M_s , $[\text{Co}/\text{Ni}/\text{Pd}]_9$ exhibits more sizeable domains, which could be a sign of a larger exchange stiffness A in Co/Ni/Pd MLs. For 15 repetitions, $[\text{Co}/\text{Ni}/\text{Pt}]_{15}$ shows slightly larger domains, which can be explained by the smaller M_s value compared to $[\text{Co}/\text{Ni}/\text{Pd}]_{15}$.

C. Curie temperatures

Furthermore, we have investigated the Curie temperature T_c for selected Co/Ni/X MLs. In order to extract T_c , the magnetization M of $[\text{Co}/\text{Ni}]_3$, $[\text{Co}/\text{Ni}]_9$, $[\text{Co}/\text{Ni}/\text{Pd}]_9$, and $[\text{Co}/\text{Ni}/\text{Pt}]_9$ was measured dependent on the temperature T (figure 7). All

systems were saturated at 300 K and afterwards measured with increasing T and an effective guiding field of 10 mT. The measurement geometry of all samples was in oop direction, except [Co/Ni]₉, which was measured in ip geometry because of its ip easy axis. T_c was estimated by the intersecting tangents method.

All $M - T$ curves, except for [Co/Ni/Pt]₉, do not drop fully to zero at their Curie temperature. Films measured oop might also lose magnetization due to decreasing K_u , which is induced by interfacial intermixing at these elevated measurement temperatures[48]. The Curie temperatures of [Co(0.2)/Ni(0.4)/Pd(0.6)]₉ and [Co(0.2)/Ni(0.4)/Pt(0.6)]₉ determined to 530 K and 560 K, respectively, are significantly lower than the $T_c = 720$ K of the [Co(0.2)/Ni(0.4)]₉ ML without insertion layers. The reduction in exchange energy caused by the insertion layers is mostly responsible for that. If we compare [Co(0.2)/Ni(0.4)]₃ to the other samples, we find a T_c of 520 K which is much lower than for the Co/Ni ML with 9 repetitions due to its smaller thickness. These values are in agreement with literature values. It was reported that T_c of Co/Pt and Co/Pd MLs lies between 520 and 570 K [62, 63] depending on the multilayer composition, while T_c of Co/Ni MLs can be as high as 950 K, similar to Co₃₃Ni₆₇ alloys [64].

IV. CONCLUSION

The influence of Pd and Pt insertion layers on the magnetic properties of Co/Ni MLs was studied. It was shown that systems with and without insertion layers have a rather similar Co thickness dependence. An optimal Co layer thickness of $t_{Co} = 0.2$ nm was validated for all systems in order to achieve strong PMA. While K_{eff} could be more than doubled, M_s and K_u decreased drastically with insertion of Pd and Pt. The repetition number study revealed that K_{eff} could be increased over the whole measured range of repetition numbers of at least up to 15, allowing for extending the transition from an oop to an ip easy axis for larger repetition numbers for samples with insertion layers. MLs with Pt as insertion layer showed the largest K_{eff} and $\mu_0 H_c$. The variation of the magnetic domain sizes are consistent with the corresponding magnetic properties of the three sample series. Furthermore, insertion of Pd and Pt decreased the Curie temperature from 720 K for [Co/Ni]₉ to 530 K and 560 K, respectively.

ACKNOWLEDGMENTS

Financial support for this project was provided by the German Research Foundation (DFG, D.A.CH project AL 618/24-1) is gratefully acknowledged.

-
- [1] S. Hashimoto, Y. Ochiai, and K. Aso, "Perpendicular magnetic anisotropy and magnetostriction of sputtered Co/Pd and Co/Pt multilayered films," *J. Appl. Phys.* **66**, 4909 (1989).
 - [2] C. Etz, J. Zabloudil, P. Weinberger and E. Y. Vedmedenko, "Magnetic properties of single atoms of Fe and Co on Ir(111) and Pt(111)," *Phys. Rev. B* **77**, 184425 (2008).
 - [3] S. Girod, M. Gottwald, S. Andrieu, S. Mangin, J. McCord, E. E. Fullerton, J. M. Beaujour, B. J. Krishnatreya, and A. D. Kent, "Strong perpendicular magnetic anisotropy in Ni/Co(111) single crystal superlattices," *Appl. Phys. Lett.* **94**, 262504 (2009).
 - [4] M. Gottwald, S. Andrieu, F. Gimbert, E. Shipton, L. Calmels, C. Magen, E. Snoeck, M. Liberati, T. Hauet, E. Arenholz, S. Mangin, and E. E. Fullerton, "Co/Ni(111) superlattices studied by microscopy, x-ray absorption, and ab initio calculations," *Phys. Rev. B* **86**, 014425 (2012).
 - [5] J. M. Beaujour, W. Chen, K. Krycka, C. C. Kao, J. Z. Sun, and A. D. Kent, "Ferromagnetic resonance study of sputtered Co/Ni multilayers," *Euro. Phys. J. B* **59**, 475 (2007).
 - [6] F. J. A. den Broeder, W. Hoving, and P. J. H. Bloemen, "Magnetic anisotropy of multilayers," *J. Magn. & Magn. Mater.* **93**, 562 (1991).
 - [7] G. H. O. Daalderop, P. J. Kelly, and F. J. A. D. Broeder, "Prediction and Confirmation of Perpendicular Magnetic Anisotropy in Co/Ni Multilayers," *Phys. Rev. Lett.* **68**, 5 (1992).
 - [8] M. Arora, R. Hübner, D. Suess, B. Heinrich, and E. Girt, "Origin of perpendicular magnetic anisotropy in Co/Ni multilayers," *Phys. Rev. B* **96**, 024401 (2017).
 - [9] S. Hashimoto and Y. Ochiai, "Co/Pt and Co/Pd multilayers as magneto-optical recoding materials," *J. Magn. Magn. Mater* **88**, 211 (1990).
 - [10] E. E. Fullerton, K. Hono, Y. Fainman, G. Malinowski, Y. K. Takahashi, B. S. D. C. S. Varaprasad, M. Cinchetti, M. Hehn, S. Mangin, C.-H. Lambert, and M. Aeschlimann, "All-optical control of ferromagnetic thin films and nanostructures," *Science* **345**, 1337 (2014).
 - [11] P. Zhang, K. Xie, W. Lin, D. Wu, and H. Sang, "Anomalous Hall effect in Co/Ni multilayers with perpendicular magnetic anisotropy," *Appl. Phys. Lett.* **104**, 082404 (2014).
 - [12] J. A. Katine and E. E. Fullerton, "Device implications of spin-transfer torques," *J. Magn. Magn. Mater.* **320**, 1217 (2008).
 - [13] J. S. Meena, S. M. Sze, U. Chand, and T. Y. Tseng, "Overview of emerging nonvolatile memory technologies," *Nanoscale Res. Lett.* **9**, 526 (2014).
 - [14] J. C. Sankey, Y. T. Cui, J. Z. Sun, J. C. Slonczewski, R. A. Buhrman, and D. C. Ralph, "Measurement of the spin-transfer-torque vector in magnetic tunnel junctions," *Nature Phys.* **4**, 67 (2008).
 - [15] L. You, R. C. Sousa, S. Bandiera, B. Rodmacq and B. Dieny, "Co / Ni multilayers with perpendicular anisotropy for spintronic device applications," *Appl. Phys. Lett.* **100**, 172411 (2012).
 - [16] S. H. Yang, K. S. Ryu, and S. Parkin, "Domain-wall velocities of up to 750 m s⁻¹ driven by exchange-coupling torque in synthetic antiferromagnets," *Nature Nanotechn.* **10**, 221 (2015).
 - [17] S. Le Gall, N. Vernier, F. Montaigne, M. Gottwald, D. Lacour, M. Hehn, D. Ravelosona, S. Mangin, S. Andrieu, and T. Hauet, "Thermally activated domain wall motion in [Co/Ni](111) superlattices with perpendicular magnetic anisotropy," *Appl. Phys. Lett.* **106**, 062406 (2015).
 - [18] T. Albrecht, H. Arora, V. Ayanoor-Vitikkate, J.-M. Beaujour, D. Bedau, D. Berman, A. Bogdanov, Y.-A. Chapuis, J. Cushen,

- E. Dobisz, G. Doerk, H. Gao, M. Grobis, B. Gurney, W. Hanson, O. Hellwig, T. Hirano, P. Jubert, D. Kercher, and E. Yang, "Bit patterned magnetic recording: Theory, media fabrication, and recording performance," *IEEE Trans. Magn.* **51**, 0800342 (2015).
- [19] T. R. Albrecht, D. Bedau, E. Dobisz, H. Gao, M. Grobis, O. Hellwig, D. Kercher, J. Lille, E. Marinero, K. Patel, R. Ruiz, M. E. Schabes, L. Wan, D. Weller, and T. Wu, "Bit patterned media at 1 tdot/in2 and beyond," *IEEE Trans. Magn.* **49**, 773 (2013).
- [20] M. Albrecht, G. Hu, I. L. Guhr, T. C. Ulbrich, J. Boneberg, P. Leiderer, and G. Schatz, "Magnetic multilayers on nanospheres," *Nature Mater.* **4**, 203 (2005).
- [21] O. Hellwig, T. Hauet, T. Thomson, E. Dobisz, J. D. Risner-Jamtgaard, D. Yaney, B. D. Terris, and E. E. Fullerton, "Coercivity tuning in Co/Pd multilayer based bit patterned media," *Appl. Phys. Lett.* **95**, 232505 (2009).
- [22] G. Varvaro, S. Laureti, D. Peddis, M. Hassan, G. Barucca, P. Mengucci, A. Gerardino, E. Giovine, O. Lik, D. Nissen, and M. Albrecht, "Co/Pd-Based synthetic antiferromagnetic thin films on Au/resist underlayers: Towards biomedical applications," *Nanoscale* **11**, 21891 (2019).
- [23] F. Gimbert, L. Calmels, and S. Andrieu, "Localized electron states and spin polarization in Co/Ni(111) overlayers," *Phys. Rev. B* **84**, 094432 (2011).
- [24] S. Andrieu, T. Hauet, M. Gottwald, A. Rajanikanth, L. Calmels, A. M. Bataille, F. Montaigne, S. Mangin, E. Otero, P. Ohresser, P. Le Fèvre, F. Bertran, A. Resta, A. Vlad, A. Coati, and Y. Garreau, "Co/Ni multilayers for spintronics: High spin polarization and tunable magnetic anisotropy," *Phys. Rev. Mater.* **2**, 064410 (2018).
- [25] H. S. Song, K. D. Lee, J. W. Sohn, S. H. Yang, S. S. Parkin, C. Y. You, and S. C. Shin, "Observation of the intrinsic Gilbert damping constant in Co/Ni multilayers independent of the stack number with perpendicular anisotropy," *Appl. Phys. Lett.* **102**, 102401 (2013).
- [26] W. Chen, J. M. L. Beaujour, G. De Loubens, A. D. Kent, and J. Z. Sun, "Spin-torque driven ferromagnetic resonance of CoNi synthetic layers in spin valves," *Appl. Phys. Lett.* **92**, 012507 (2008).
- [27] L. Ertl, G. Endl, and H. Hoffmann, "Structure and magnetic properties of sputtered Tb/Co multilayers," *J. Magn. Magn. Mater.* **113**, 227 (1992).
- [28] T. Seki, J. Shimada, S. Iihama, M. Tsujikawa, T. Koganezawa, A. Shioda, T. Tashiro, W. Zhou, S. Mizukami, M. Shirai, and K. Takahashi, "Magnetic anisotropy and damping for monolayer-controlled Co | Ni epitaxial multilayer," *J. Phys. Soc. Japan* **86**, 074710 (2017).
- [29] M. T. Johnson, P. J. H. Bloemen, F. J. A. den Broeder, and J. J. de Vries, "Magnetic anisotropy in metallic multilayers," *Rep. Prog. Phys.* **59**, 1409 (1996).
- [30] D. Sander, "The magnetic anisotropy and spin reorientation of nanostructures and nanoscale films," *J. Phys. Condens. Mater.* **16**, R603 (2004).
- [31] M. Sakamaki, K. Amemiya, M. O. Liedke, J. Fassbender, P. Mazalski, I. Sveklo, and A. Maziewski, "Perpendicular magnetic anisotropy in a Pt/Co/Pt ultrathin film arising from a lattice distortion induced by ion irradiation," *Phys. Rev. B* **86**, 024418 (2012).
- [32] C. R. Chang, "Magnetostrictive surface anisotropy of epitaxial multilayers," *Phys. Rev. B* **48**, 15817 (1993).
- [33] G. H. O. Daalderop, P. J. Kelly and M. F. H. Schuurmans, "First-principles calculation of the magnetic anisotropy energy of (Co)_n(X)_n multilayers," *Phys. Rev. B* **42**, 7270 (1990).
- [34] F. den Broeder, E. Janssen, W. Hoving, and W. Zeper, "Perpendicular Magnetic Anisotropy and Coercivity of Co/Ni Multilayers," *IEEE Trans. Magn.* **28** (1992).
- [35] P. J. H. Bloemen, W. J. M. De Jonge, and F. J. A. Den Broeder, "Magnetic anisotropies in Co/Ni(111) multilayers," *J. Appl. Phys.* **72**, 4840 (1992).
- [36] P. F. Carcia, "Perpendicular magnetic anisotropy in Pd/Co and Pt/Co thin-film layered structures," *J. Appl. Phys.* **63**, 5066 (1988).
- [37] J. W. Knepper and F. Y. Yang, "Oscillatory interlayer coupling in Co Pt multilayers with perpendicular anisotropy," *Phys. Rev. B* **71**, 209 (2005).
- [38] S. Akbulut, A. Akbulut, M. Özdemir, and F. Yildiz, "Effect of deposition technique of Ni on the perpendicular magnetic anisotropy in Co/Ni multilayers," *J. Magn. Magn. Mater.* **390**, 137 (2015).
- [39] O. Posth, C. Hassel, M. Spasova, G. Dumpich, J. Lindner, and S. Mangin, "Influence of growth parameters on the perpendicular magnetic anisotropy of [Co/Ni] multilayers and its temperature dependence," *J. Appl. Phys.* **106**, 023919 (2009).
- [40] E. Liu, J. Swerts, T. Devolder, S. Couet, S. Mertens, T. Lin, V. Spampinato, A. Franquet, T. Conard, S. Van Elshocht, A. Furnemont, J. De Boeck, and G. Kar, "Seed layer impact on structural and magnetic properties of [Co/Ni] multilayers with perpendicular magnetic anisotropy," *J. Appl. Phys.* **121** (2017).
- [41] Y. B. Zhang and J. a. Woollam, "Annealing Effects of Co/Ni Multilayers," *IEEE Trans. Magn.* **31**, 3262 (1995).
- [42] H. Kurt, M. Venkatesan, and J. M. Coey, "Enhanced perpendicular magnetic anisotropy in Co/Ni multilayers with a thin seed layer," *J. Appl. Phys.* **108**, 073916 (2010).
- [43] D. Stanesco, D. Ravelosona, V. Mathet, C. Chappert, Y. Samson, C. Beigné, N. Vernier, J. Ferf, J. Gierak, E. Bouhris, and E. Fullerton, "Tailoring magnetism in CoNi films with perpendicular anisotropy by ion irradiation," *J. Appl. Phys.* **103**, 07B529 (2008).
- [44] C. Schuppler, A. Habenicht, I. L. Guhr, M. Maret, P. Leiderer, J. Boneberg, and M. Albrecht, "Control of magnetic anisotropy and magnetic patterning of perpendicular Co/Pt multilayers by laser irradiation," *Appl. Phys. Lett.* **88**, 012506 (2006).
- [45] T. C. Ulbrich, D. Assmann, and M. Albrecht, "Magnetic properties of Co/Pt multilayers on self-assembled particle arrays," *J. Appl. Phys.* **104**, 084311 (2008).
- [46] N. Nakajima, T. Koide, T. Shidara, H. Miyauchi, H. Fukutani, A. Fujimori, K. Iio, T. Katayama, M. Nývlt, and Y. Suzuki, "Perpendicular Magnetic Anisotropy Caused by Interfacial Hybridization via Enhanced Orbital Moment in Co/Pt Multilayers: Magnetic Circular X-Ray Dichroism Study," *Phys. Rev. Lett.* **81**, 5229 (1998).
- [47] W. B. Zeper, F. J. A. M. Greidanus, P. F. Carcia, and C. R. Fincher, "Perpendicular magnetic anisotropy and magneto-optical Kerr effect of vapor-deposited Co/Pt-layered structures," *J. of Appl. Phys.* **65**, 4971 (1989).
- [48] X. Chen, M. Li, K. Yang, S. Jiang, and G. Han, "Large enhancement of perpendicular magnetic anisotropy and high annealing stability by Pt insertion layer in (Co/Ni)_n-based multilayers," *AIP Advances* **5**, 097121 (2015).
- [49] A.-o. Mandru, O. Yildirim, M. A. Marioni, H. Rohrmann, M. Heigl, T. Ciubotariu, M. Penedo, X. Zhao, M. Albrecht, and H. J. Hug, "Pervasive artifacts revealed from magnetometry measurements of rare earth-transition metal thin films," *J. Vac. Sci. Tec. A* **38**, 023409 (2020).
- [50] S. Bandiera, R. R. Sousa, B. B. Rodmacq, and B. Dieny, "Asymmetric interfacial perpendicular magnetic anisotropy in pt/co/pt trilayers," *IEEE Magn. Lett.* **2**, 3000504 (2011).

- [51] J. M. D. Coey, *Magnetism and Magnetic Materials* (Cambridge University Press, 2010).
- [52] P. Srivastava, F. Wilhelm, A. Ney, M. Farle, H. Wende, N. Haack, G. Ceballos, and K. Baberschke, "Magnetic moments and Curie temperatures of Ni and Co thin films and coupled trilayers," *Phys. Rev. B* **58**, 5701 (1998).
- [53] C. C. D. Weller, Y. Wu, J. Stohr, and M. G. Samant, B. D. Hermsmeier, "Orbital magnetic moments of Co in multilayers with perpendicular magnetic anisotropy," *Phys. Rev. B* **49**, 888 (1994).
- [54] K. Chafai, H. Salhi, H. Lassri, Z. Yamkane, M. Lassri, M. Abid, E. K. Hlil, and R. Krishnan, "Magnetic studies in evaporated Ni/Pd multilayers," *J. Magn. Magn. Mater.* **323**, 596 (2011).
- [55] K. Benkirane, R. Elkabil, M. Lassri, M. Abid, H. Lassri, A. Berrada, A. Hamdoun, and R. Krishnan, "Magnetic properties of Ni/Pt multilayers," *Mater. Sci. Eng. B* **116**, 25 (2005).
- [56] X. T. Tang, G. C. Wang, and M. Shima, "Superparamagnetic behavior in ultrathin CoNi layers of electrodeposited CoNi/Cu multilayer nanowires," *J. Appl. Phys.* **99**, 15 (2006).
- [57] B. Kaplan and G. A. Gehring, "The domain structure in ultrathin magnetic films," *J. Magn. Magn. Mater.* **128**, 111 (1993).
- [58] J. P. Pellegrin, D. Lau, and V. Sokalski, "Dispersive Stiffness of Dzyaloshinskii Domain Walls," *Phys. Rev. Lett.* **119**, 027203 (2017).
- [59] F. MacIà, P. Warnicke, D. Bedau, M. Y. Im, P. Fischer, D. A. Arena, and A. D. Kent, "Perpendicular magnetic anisotropy in ultrathin Co | Ni multilayer films studied with ferromagnetic resonance and magnetic x-ray microspectroscopy," *J. Magn. Magn. Mater.* **324**, 3629 (2012).
- [60] S. Al Risi, S. Bhatti, A. Al Subhi, S. N. Piramanayagam, and R. Sbiaa, "Magnetic domain structure and magnetization reversal in (Co/Ni) and (Co/Pd) multilayers," *Journal of Magnetism and Magnetic Materials* **503**, 166579 (2020).
- [61] X. Wang, W. Yurui, K. He, Y. Liu, Y. Huang, Q. Liu, J. Wang, and G. Han, "Effect of the repeat number and Co layer thickness on the magnetization reversal process in [Pt/Co(x)]N multilayers," *J. Phys. D: Appl. Phys.* **53**, 215001 (2020).
- [62] F. J. A. den Broeder, H. W. van Kesteren, W. Hoving and W. B. Zeper, "Co / Ni multilayers with perpendicular magnetic anisotropy : Kerr effect and thermomagnetic writing," *Appl. Phys. Lett.* **61**, 1468 (1992).
- [63] P. Carcia, W. Zeper, H. van Kesteren, B. Jacobs, and J. Spruit, "Materials' Challenges for Metal Multilayers As a Magneto-Optical Recording Medium," *J. Magn. Soc. Japan* **15**, 151 (1991).
- [64] M. Hansen, K. Anderko, and H. W. Salzberg, *Constitution of Binary Alloys* (New York, McGraw-Hill).